

Optimization of Superconducting Hot-Electron Sensors: Controlling of Electron-Phonon Relaxation

A. Sergeev and V. Mitin.

Department of ECE, Wayne State University, Detroit, MI 48202

Abstract

Electron scattering from boundaries and impurities destroys the single-particle picture of the electron-phonon interaction. We show that quantum interference between 'pure' electron-phonon and electron-boundary/impurity scattering may result in the enlargement as well as to the significant reduction of the electron relaxation time. This effect crucially depends on the extent, to which electron scatterers are dragged by phonons. Static and vibrating scatterers may be described by two dimensionless parameters $q_T l$ and $q_T L$, where q is the wave vector of the thermal phonon, l is the total electron mean free path, L is the mean free path due to scattering from static scatterers. According to Pippard, without static scatterers the relaxation rate is $1/ql$ slower than the rate in pure bulk material. However, in the presence of static potential the relaxation rate turns out to be $1/qL$ times faster. Thus, at low temperatures, electron energy relaxation may be controlled in a wide range. For instance, we expect that the possible variation of the electron relaxation time at 100 mK spans the interval from 10^{-6} to 0.1 s. Slow relaxation allows us to reach values of NEP of direct resistive detectors as small as 10^{-21} - 10^{-20} W/Hz^{1/2} at 100 mK.

Introduction

The idea of a superconducting hot-electron sensor was proposed more than 15 years ago [1]. In such sensor (for a review see [2]), the radiation overheats only electrons in a superconducting film driven by the current (magnetic field) in a resistive state. The phonons in the film remain in equilibrium with the substrate and play the role of a heat sink for electrons. Thus, the electron-phonon interaction is a bottleneck for the heat transfer from electrons to the heat sink. This regime is achieved by increasing the thermal conductance between the superconducting structure and the environment, opposite to the case of conventional bolometers. The characteristic time of the sensor is determined by the inelastic electron-phonon scattering time. The sensitivity is limited by the fluctuations of electron parameters (electron temperature, quasiparticle chemical potential). High quantum efficiency is reached due to strong electron-electron interaction in disordered conductors. The figure-of-merit of the hot-electron sensor depends only on the heat capacity of electrons (quasiparticles), while in conventional bolometers there is additional large heat capacity of the whole detector. Therefore, the hot-electron sensor offer the best figure-of-merit of any type of bolometers.

Up to now, fast hot-electron detectors with characteristic time 0.1-10 ns operating at helium temperatures have been well developed and are used as broadband mixers. With controllable slow relaxation of hot electrons (quasiparticles) and due to small electron heat capacity, hot-electron superconducting sensors are very promising to use as ultrasensitive resistive detectors and quantum calorimeters. We present new concepts of controlling parameters of hot-electron sensors. The sensitivity of direct detectors

and quantum calorimeters may be significantly improved in comparison with the sensitivity of traditional bolometric devices.

Electron-phonon relaxation rate is controlled by the quantum interference between 'pure' electron-phonon and electron-boundary/impurity scattering [3]. The interference may result in the enlargement as well as to the significant reduction of the electron-phonon relaxation time. This effect crucially depends on the extent, to which electron scatterers, such as boundaries and impurities, are dragged by phonons. Static and vibrating scatterers may be described by two dimensionless parameters $q_T l$ and $q_T L$, where q_T is the wave vector of the thermal phonon, l is the total electron mean free path, and L is the mean free path due to scattering from static scatterers. Without static scatterers the relaxation rate is $1/ql$ slower than the rate in pure bulk material. However, in the presence of static potential the electron-phonon relaxation rate turns out to be $1/qL$ times faster. Slow relaxation allows one to reach record values of sensitivity [4]. Due to unique sensitivity, direct detectors and quantum calorimeters based on electron heating may be successfully employed for many astrophysical measurements of weak electromagnetic radiation and energy of particles.

Pippard ineffectiveness condition

In recent years, the electron relaxation and dephasing in ultrathin films, nanostructures and mesoscopic devices has been intensively studied. Note, that the temperature-dependent dephasing rate is mainly determined by the electron-electron and electron-phonon interactions. While theoretical results pertaining to electron-electron scattering are confirmed by many experiments, the electron-phonon scattering mechanism is still poorly understood. Unfortunately, most researchers employ the standard clean-limit concept, its uncritical application leads to incorrect and controversial conclusions. A reliable electron-phonon interaction model taking into account electron scattering from boundaries, defects and impurities is of vital importance.

If scattering potential of boundaries and impurities is completely dragged by phonons, the inelastic electron scattering from this potential may be excluded by a transformation to the frame, which moves together with the phonon. In other words, in this case the local lattice velocity plays a role of the hydrodynamical variable. Using transformation to the local frame, Pippard has found that the electron-phonon coupling depends essentially on the parameter ql , where q is the wave vector of a phonon, and l is the electron mean free path. If $ql < 1$, the electron-phonon coupling is a factor of ql weaker than the coupling in the pure limit, $l \rightarrow \infty$. This statement is well known as the Pippard ineffectiveness condition [6, 7]. It was confirmed by microscopic calculations in [8].

Obviously the Pippard's assumption about completely dragged scatterers is not valid in micro and nanostructures. The electron scattering from boundaries and defects with a mass different from a mass of host atoms significantly changes effective electron-phonon interaction. To generalize the Pippard's model we take into account additional static potential. We show that even relatively weak static potential drastically changes the effective electron-phonon coupling and corresponding electron dephasing rate.

Model

We start with the Hamiltonian, which describes the 'pure' electron-phonon interaction and the interaction between electrons and scatterers that are completely dragged by phonons [8, 10],

$$\begin{aligned}
 H_{int} &= \sum_{\mathbf{p}, \mathbf{q}} g(\mathbf{q}) c_{\mathbf{p}+\mathbf{q}}^{\dagger} c_{\mathbf{p}} (b_{\mathbf{q}, n} + b_{-\mathbf{q}, n}^{\dagger}) + \sum_{\mathbf{p}, \mathbf{k}, \mathbf{R}_{\alpha}} V(\mathbf{k}) c_{\mathbf{p}}^{\dagger} c_{\mathbf{p}-\mathbf{k}} \exp(-i\mathbf{k}\mathbf{R}_{\alpha}) \\
 &+ \sum_{\mathbf{p}, \mathbf{k}, \mathbf{q}, \mathbf{R}_{\alpha}} \gamma(\mathbf{k}, \mathbf{q}) c_{\mathbf{p}}^{\dagger} c_{\mathbf{p}-\mathbf{k}} (b_{\mathbf{q}, n} + b_{-\mathbf{q}, n}^{\dagger}) \exp[-i(\mathbf{k} - \mathbf{q})\mathbf{R}_{\alpha}],
 \end{aligned} \tag{1}$$

where $c_{\mathbf{p}}^{\dagger}$ is the electron creation operator, $b_{\mathbf{q}, n}^{\dagger}$ is the creation operator of a phonon with a wave vector \mathbf{q} and polarization index n , and \mathbf{R}_{α} are the equilibrium positions of scatterers.

The vertex of pure phonon-electron scattering is given by

$$g = \frac{2\epsilon_F}{3} \frac{\mathbf{q} \cdot \mathbf{e}_n}{(2\rho\omega)^{1/2}}, \tag{2}$$

where ϵ_F is the Fermi energy, \mathbf{e}_n is the phonon polarization vector, ρ is the density.

The second term describes elastic electron scattering from the scattering potential V . If this potential is completely dragged by phonons, the vertex of inelastic electron scattering is given by [9]

$$\gamma(\mathbf{k}, \mathbf{q}) = -iV(\mathbf{k}\mathbf{e}_n)/(2\rho\omega_q)^{1/2}, \quad (3)$$

The inelastic electron scattering is characterized by a large value of the electron momentum transferred to impurity ($k \sim p_F$), while the transferred energy is the same as in the pure phonon-electron interaction.

We will assume that the potential V is δ -correlated random potential. Then the electrical resistivity determined by the Hamiltonian in the form of eq. (1) is

$$\rho(T) = \rho_0 + \rho_{BG}(T) + \rho_{int}(T), \quad (4)$$

where ρ_0 is the residual resistivity due to elastic electron scattering, ρ_{BG} is the Bloch-Grüneisen term due to the pure electron-phonon scattering. The interference term, ρ_{int} , is determined by the inelastic electron scattering and quantum nonequilibrium corrections to the processes of pure electron-phonon scattering [10]. If $T > u/l$, the interference term has a form: $\rho_{int} = B\rho_0 T^2$, the longitudinal phonons give a negative correction to the resistivity, while the transverse phonons result in a positive correction [10].

Now take into account the static scatterers (rigid boundaries and heavy defects). Then the total momentum relaxation rate ($1/\tau$) is determined by

$$\tau^{-1} = \tilde{\tau}^{-1} + \tau_{qs}^{-1}, \quad (5)$$

where $1/\tilde{\tau}$ is the electron momentum relaxation rate due to scatterers that are dragged by phonons, and $1/\tau_{qs}$ is the relaxation rate due to static scatterers. It is convenient to introduce the electron mean free path, $l = v_F\tau$, and the electron free path with respect to scattering from static potential, $L = V_F\tau$. As we will see, the modification of the electron dephasing rate crucially depends on the parameter l/L .

Electron Relaxation Rate

The electron-phonon collision integral taking into account the interference between different channels of electron scattering may be obtained by means of the Keldysh diagrammatic technique for nonequilibrium processes. Cumbersome calculations will be presented elsewhere. The collision integral, which describes the interaction between longitudinal phonons and electrons in a disordered conductor with static and vibrating scattering potentials is given by

$$I_{e-l.ph}(\epsilon) = -\frac{\beta_l T^3}{(p_F u_l)^2} \int d\omega_q R(\epsilon, \omega_q) \left[\frac{ql\zeta_0}{1-\zeta_0} - \left(1 - \frac{l}{L}\right) \frac{3}{(ql)^2} \right], \quad (6)$$

where $\zeta_0 = \arctan(ql)/(ql)$, the dimensionless constant of the electron-phonon interaction $\beta_l = (2\epsilon_F/3)^2 \nu / 2\rho u_l^2$ (u_l is the longitudinal sound velocity), and $R(\epsilon, \omega_q)$ is the combination of electron (n_ϵ) and phonon (N_ω) distribution functions,

$$R(\epsilon, \omega) = N_\omega n_\epsilon (1 - n_{\epsilon+\omega}) - (1 + N_\omega)(1 - n_\epsilon) n_{\epsilon+\omega}. \quad (7)$$

The electron relaxation rate is determined as

$$\frac{1}{\tau_{e-ph}(\epsilon)} = -\frac{\delta I_{ph-e}}{\delta n_\epsilon} (n_\epsilon = n_\epsilon^{eq}), \quad (8)$$

where n_ϵ^{eq} is the equilibrium distribution function.

Finally, the energy relaxation rate of electrons interacting with longitudinal phonons is

$$\frac{1}{\tau_{e-l.ph}(0)} = \frac{7\pi\zeta(3)}{2} \frac{\beta_l T^3}{(p_F u_l)^2} F_l(q_T l), \quad (9)$$

$$F_l(z) = \frac{2}{7\zeta(3)} \int_0^{A_l} dx \Phi_l(xz) (N_x + n_x) x^2, \quad (10)$$

$$\Phi_l(x) = \frac{2}{\pi} \left(\frac{x \arctan(x)}{x - \arctan(x)} - \frac{3}{x} \frac{\tau}{\tilde{\tau}} \right), \quad (11)$$

where $A_{t(l)} = \theta_D l / u_{t(l)} z$ (θ_D is the Debye temperature). In the limiting cases the relaxation rate is given by

$$\frac{1}{\tau_{e-l.ph}(0)} = \frac{7\pi\zeta(3)}{2} \frac{\beta_l T^3}{(p_F u_l)^2} \text{times} \begin{cases} 1, & Tl > u_l, \\ \frac{2\pi^3}{35\zeta(3)} \frac{Tl}{u_l} + \frac{3\pi}{7\zeta(3)} \frac{u_l}{TL}, & Tl < u_l. \end{cases} \quad (12)$$

Now we consider interaction of electrons and transverse phonons. The corresponding collision integral has a form

$$I_{e-t.ph}(\epsilon) = \frac{3\pi^2 \beta_l T^2}{(p_F u_t)(p_F l)} \left(1 - \frac{l}{L}\right) \int d\omega_q R(\epsilon, \omega_q) \left[1 + \left(1 - \frac{l}{L}\right) \frac{3x - 3(x^2 + 1) \arctan(x)}{2x^3}\right], \quad (13)$$

where the dimensionless constant is $\beta_t = \beta_l (u_l / u_t)^2$, and u_t is the transverse sound velocity. Then the electron relaxation rate is

$$\frac{1}{\tau_{e-t.ph}(0)} = \frac{3\pi^2 \beta_l T^2}{p_F^2 u_t} \left(\frac{1}{l} - \frac{1}{L}\right) F_t(q_T l), \quad (14)$$

$$F_t(z) = \frac{4}{\pi^2} \int_0^{A_t} dx \Phi_t(xz) (N_x + n_x^{\epsilon q}) x, \quad (15)$$

$$\Phi_t(x) = 1 + \left(1 - \frac{l}{L}\right) \frac{3x - 3(x^2 + 1) \arctan(x)}{2x^3}. \quad (16)$$

In the limiting cases the electron relaxation rate is

$$\frac{1}{\tau_{e-t.ph}(0)} = \frac{3\pi^2 \beta_l T^2}{p_F^2 u_t} \left(\frac{1}{l} - \frac{1}{L}\right) \times \begin{cases} 1, & Tl > u_t, \\ \frac{l}{L} + \left(1 - \frac{l}{L}\right) \frac{\pi^2}{10} \left(\frac{Tl}{u_t}\right)^2, & Tl < u_t. \end{cases} \quad (17)$$

Therefore, in the impure case ($Tl < u_l, u_t$), the electron-phonon scattering rate is given by

$$\frac{1}{\tau_{e-ph}(0)} = \frac{\pi^4 T^4}{5} (p_F l) \left[\frac{\beta_l}{(p_F u_l)^3} + \frac{3\beta_t}{2(p_F u_t)^3} \left(1 - \frac{l}{L}\right) \right] + \frac{3\pi^2 T^2}{2p_F L} \left[\frac{\beta_l}{p_F u_l} + \frac{2\beta_t}{p_F u_t} \left(1 - \frac{l}{L}\right) \right].$$

Discussion

Presence of static and vibrating electron scatterers leads to complex quantum interference between different scattering mechanisms. If boundaries, defects and impurities are completely dragged by phonons ($L \rightarrow \infty$), we reproduce results of Ref. 9 for electron-relaxation rate. In agreement with the Pippard ineffectiveness condition, at low temperatures the electron-phonon relaxation rate is $u/(Tl)$ times slower than the rate in a pure conductor. Note, that in our model with spherical Fermi surface, in the pure conductor only longitudinal phonons interact with electrons. Transverse phonons may interact with electrons due to vibrating boundaries and impurities, which generate a new channel of the electron-phonon interaction. In the limit $Tl/u \gg 1$, this channel is Tl/u times weaker than the pure electron-phonon interaction. In limit $Tl/u \ll 1$, both channels are enhanced due to the diffusion electron motion. However, due to the quantum interference, strong scattering processes cancel each other. Obtained by many authors [11], conclusion about enhancement of the electron-phonon interaction due to disorder in the frame of the Pippard model is wrong.

This picture is changed in the presence of additional static potential (or due to incomplete drag of boundaries and impurities by phonons). In the limit $Tl/u \ll 1$, where the interference is important, the electron relaxation rate turns out to be $u/(TL)$ times faster than the rate in the pure conductor. Note, that the relaxation rate due to transverse phonons consists of the large factor $(u_l/u_t)^3$ and the factor $(1 - l/L)$ compared with the relaxation effect of longitudinal phonons. The factor $(1 - l/L)$ has a simple interpretation: it is proportional to the concentration of vibrating scatterers, which provide the interaction between electrons and transverse phonons. If this factor is not too small, the effect of transverse phonons dominates at low temperatures.

To illustrate our results, we calculate the electron relaxation rate in Al structures. Parameters of Al are $u_l = 3.2 \cdot 10^5$ cm/s, $u_t = 1.2 \cdot 10^5$ cm/s, $v_F = 14 \cdot 10^7$ cm/s, $\beta_l = 0.2$, and $\beta_t = 1.4$. Temperature dependences of the relaxation rate in the structures with the electron mean free path $0.05 \mu\text{m}$ and $0.005 \mu\text{m}$ are presented in figs. 1 and 2. Solid lines show the relaxation rate under the Pippard ineffectiveness condition. At low temperatures the relaxation becomes faster in the presence of the static potential. Comparing figs. 1 and 2, we see that at low temperatures the electron relaxation is determined by transverse phonons.

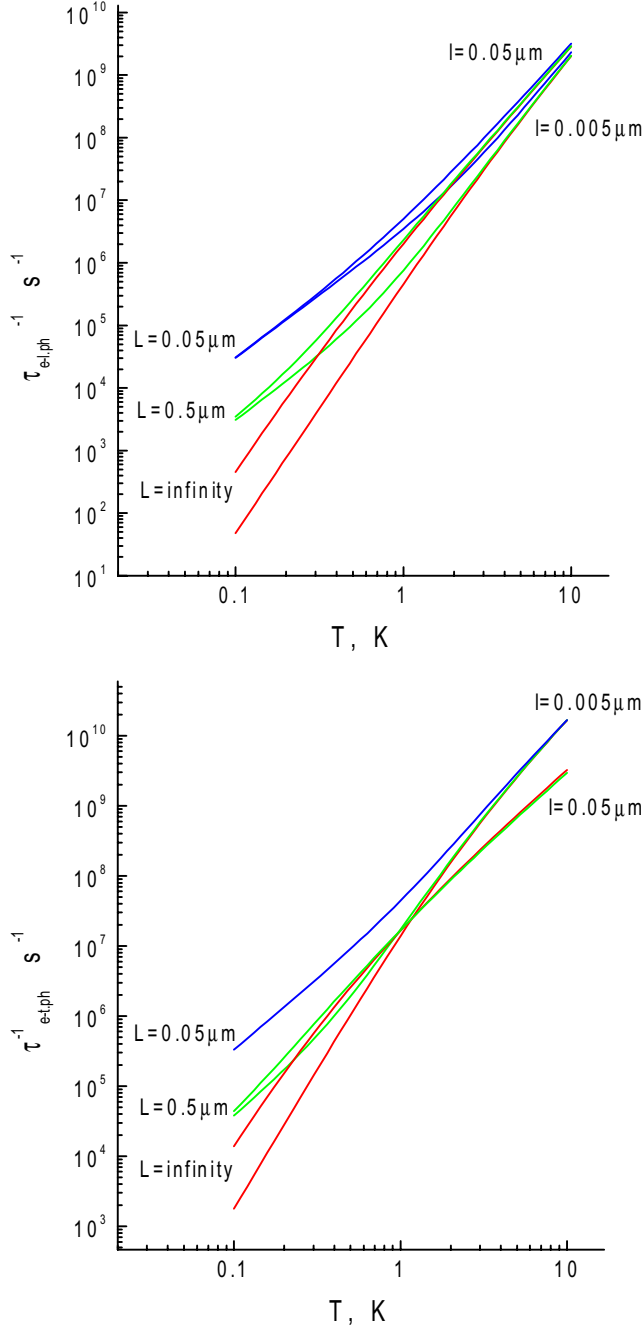


Fig. 1 and 2. Electron relaxation rate due to longitudinal (Fig. 1) and transverse (Fig. 2) phonons in Al structures with electron mean free path $l=0.005 \mu\text{m}$ and $0.05 \mu\text{m}$. Solid lines correspond to complete drag of all scatterers (boundaries and impurities) by phonons. Dashed and dotted lines correspond to the electron mean free path with respect to the static potential $L=0.05 \mu\text{m}$ and $0.5 \mu\text{m}$.

Fig. 3 shows the dependence of the relaxation rate on the electron mean free path. In the case of complete drag of boundaries and defects, the relaxation rate is proportional to l at low temperatures. In the presence of the static potential, the relaxation rate is determined mainly by the electron mean free path with respect to scattering from this potential.

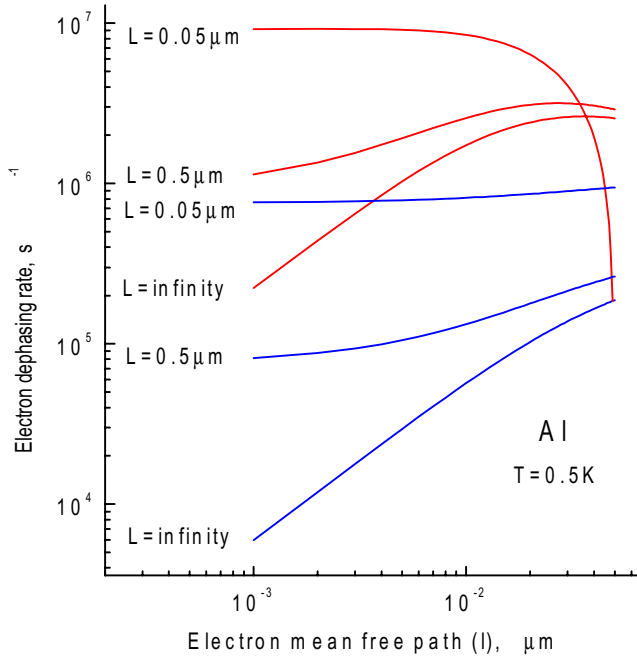


Fig. 3. Dependence of the relaxation rate on the electron mean free path. Solid and dotted lines present contributions of longitudinal and transverse phonons.

It is important for applications, that the electron-phonon scattering rate in micro and nanodevices may be changed in a wide range. It can be increased or decreased compared to the rate in a pure bulk material. For instance, we expect that the possible variation of the electron relaxation time at 100 mK spans the interval from 10^{-6} to 0.1 s. Slow relaxation allows us to reach values of NEP of direct resistive detectors as small as $10^{-21} - 10^{-20}$ W/Hz $^{1/2}$ at 100 mK [4].

Some experimental data support our conclusions. The enhancement of the electron-phonon interaction due to disorder has been found in thin metallic films [12] and semiconducting heterostructures [13]. The T^2 -dependence of the electron-phonon relaxation rate is widely observed in experiments [14]. The T^4 -dependence has been found in hafnium films on sapphire substrates. We speculate that the last result is due to very good acoustic matching of hafnium and sapphire.

Some important points, such as the modification of the phonon spectrum and vibrations of boundaries and defects, deserve further theoretical investigations. Complex measurements of the relaxation rate and parameters of electron scatterers are also very desirable.

References

- [1] E.M. Gershenson et. al., *JETP Lett.* **36**, 297 (1982); *JETP1*. E.M. Gershenson et. al., *JETP Lett.* **36**, 297 (1982); *JETP* **59**, 442 (1984); *Solid State Commun.* **50**, 207 (1984).
- [2] A.V. Sergeev and M.Yu. Reizer, *Int. J. Mod. Phys. B* **10**, 635-665 (1996).
- [3] A. Sergeev and V. Mitin, "Electron-phonon interaction in disordered conductors: static and vibrating scattering potentials", *Phys. Rev. B* **61**, 6041 (2000).

- [4] B. Karasik, W.R. McGrath, M.E. Gershenson and A.V. Sergeev, "Photon-noise limited direct detector based on disorder-controlled electron heating", accepted to *J. Appl. Phys.*
- [5] I.G. Gogidze, P.B. Kuminov, A.V. Sergeev and E.M. Gershenson, "Possibility of fabricating an inductive high-speed detector of electromagnetic radiation using YBaCuO films", *Tech.Phys.Lett.* **25**, 47 (1999).
- [6] A.B. Pippard, *Philos. Mag.* **46**, 1104 (1955).
- [7] J.M. Ziman, *Electrons and Phonons* (Clarendon, Oxford), p. 213, 1960.
- [8] G. Grünvald and K. Scharnberg, *Z. Phys.* **268**, 197 (1974).
- [9] J. Rammer and A. Schmid, *Phys. Rev. B* **34**, 1352 (1986).
- [10] M.Yu. Reizer and A.V. Sergeev, *Zh. Exsp. Teor. Fiz.* **92**, 2291 (1987) [*Sov. Phys. JETP* **65**, 1291 (1987)]; N.G. Ptitsina, G.M. Chulkova, K.S. Il'in et. al, *Phys. Rev. B* **56**, (1997) 10089.
- [11] G. Bergman, *Phys. Rev. B* **3**, 3797 (1971); H. Takayama, *Z. Phys.* **263**, 329 (1973); S.G. Lisitsin, *Sov. J. Low Temp. Phys.* **1**, 728 (1975); S.J. Poon and T.H. Geballe, *Phys. Rev. B* **18**, 233 (1978).
- [12] J.J. Lin and C.Y. Wu, *Europhys. Lett.* **29**, 141 (1995).
- [13] A. Mittal, R.G. Wheeler, M.W. Keller, D.E. Prober, and R.N. Sacks, *Surf. Science* **361-362**, 537 (1996).
- [14] G. Bergmann, *Phys. Rep.* **107**, 1 (1984).
- [15] M.E. Gershenson, D. Gong, T. Sato, B.S. Karasik, W.R. McGrath, and A.V. Sergeev, this issue.